

Empirical Line Parameters of NH_3 from 4791 to 5294 cm^{-1}

L. R. Brown and J. S. Margolis

Jet Propulsion Laboratory
California institute of Technology
Pasadena, CA 91109

Manuscript pages 13

Figures 3

Tables 9

ABSTRACT

To support remote sensing of planetary atmospheres at $2\ \mu\text{m}$, laboratory spectra of NH_3 and enriched $^{14}\text{NH}_3$ and $^{15}\text{NH}_3$ were recorded at $0.011\ \text{cm}^{-1}$ resolution with the McMath Fourier transform spectrometer (FTS) located at Kitt Peak National Observatory/ National Solar Observatory. Multiple optical paths and pressures were used with sample temperatures between 297 and 185 K. Some 2000 line positions and intensities at room temperature were measured with precision of $0.0003\ \text{cm}^{-1}$ and 3%, respectively, for unblended transitions. Low and room temperature intensities were then combined to determine empirical lower state energies for 1815 lines. These data permitted the assignments for $\nu_1 + \nu_4$ of $^{14}\text{NH}_3$ to be extended to $J' = 10$. Transitions of $\nu_3 + \nu_4$ of $^{15}\text{NH}_3$ was also cataloged for the first time. Nearly 45% of the 2000 measured features were identified, and empirical upper state levels were obtained. The experimental results for lines with measured intensities greater $3 \times 10^{-24}\ \text{cm}^{-1}/(\text{molecule} \cdot \text{cm}^{-2})$ were included to the 1996 HITRAN database. To obtain consistent NH_3 line positions, the positions of 28 H_2O transitions between 5206 and $5396\ \text{cm}^{-1}$ were also calibrated using the 2-0 band of CO at $4260\ \text{cm}^{-1}$.

INTRODUCTION

The 2 μm spectrum of ammonia contains transitions from the ground state to many vibrational states (such as $\nu_1 + \nu_4$, $\nu_3 + \nu_4$, $\nu_1 + 2\nu_2$, $2\nu_2 + \nu_3$, $4\nu_2 + \nu_4$, $2\nu_2 + 2\nu_4$, and $3\nu_4$), but only the two strongest bands have been studied at higher resolution following an initial interpretation of the vibrational spectrum in 1957 by Benedict and Plyler¹. In 1977, Sarangi measured 2100 line positions² and 412 line intensities with accuracies of 0.004 cm^{-1} and 10%, respectively, using grating spectra recorded at 0.06 cm^{-1} resolution from 4803 to 5315 cm^{-1} . He thoroughly assigned the perpendicular transitions of the strongest band, $\nu_3 + \nu_4$ near 5050 cm^{-1} . In 1989, as part of an effort to interpret NH_3 vibrational states between 4800 and 18000 cm^{-1} , Coy and Lehmann⁴ located 119 transitions involving 58 upper state levels up to $J = 7$ in the second strongest band, $\nu_1 + \nu_4$ near 4950 cm^{-1} . The other overtone and combination bands at 2 μm were not identified, and the results of these studies were never included in the HITRAN⁵ and GEISA⁶ databases,

To satisfy the needs of planetary studies with the Galileo spacecraft, the present study repeated the Sarangi measurements to provide all the required ammonia line parameters at 2 μm . Spectra were obtained with different optical paths so that line intensities could be measured at room temperatures through three orders of magnitude. Additional spectra at reduced sample temperatures were recorded, and the lower state transition energies of 90% of the lines were estimated from the temperature dependence of the intensities. In all, 2000 spectra features were measured between 4791 and 5294 cm^{-1} . The past^{2,4} analyses were extended to assign 45% of the observed features to $\nu_1 + \nu_4$ and

$\nu_3 + \nu_4$ of $^{14}\text{NH}_3$ and to $\nu_3 + \nu_4$ of $^{15}\text{NH}_3$. Empirical upper state levels were formed so that the formidable task of modeling this region by quantum mechanics can be pursued in the future. In the interim, a substantial catalog of ammonia at $2\ \mu\text{m}$ is now available on the 1996 HITRAN molecular database.

EXPERIMENTAL DETAILS and DATA REDUCTION

The laboratory data were recorded at $0.011\ \text{cm}^{-1}$ resolution using the McMath Fourier transform spectrometer (FTS) located at Kitt Peak National Observatory / National Solar Observatory. Two matched InSb detectors monitored the infrared signal from a globar source in the $3000\text{--}8800\ \text{cm}^{-1}$ region. Most spectra were acquired during an integration time of one hour with signal to noise ratios of nearly 1000:1. Five different stainless steel absorption cells were used over a period of three years; the gas conditions of the 16 room temperature and 13 cold temperature data are shown in **Table 1**. The single pass cells of 0.25, and 1.5 m and the 6 meter base multiple-pass cell at Kitt Peak were used for the room temperature data (like the spectrum shown in Figure 1). For the cold temperature data, the 0.8 m straight-pass cell and the 1. m base multiple-pass cell were transported from JPL to achieve sample temperatures down to 185 K. A few room temperature scans were recorded with the cold cells to check data consistency. Gas pressures and temperatures were monitored continually during scanning with capacitance manometers and thermistors, respectively. Two cells were sometimes used at the same time to calibrate ammonia line

centers against the 2 - 0 band of CO. The spectra usually contained absorption from residual 1120 inside the FTS, and the positions of these extra features near $1.9\ \mu\text{m}$ were also calibrated. The gas samples in the shorter path cells were enriched 99.9% $^{14}\text{NH}_3$ or 99.0% $^{15}\text{NH}_3$ while the long-path data were obtained using isotopically normal ammonia. All samples were introduced into the absorption chambers without purification.

Line positions and intensities were retrieved from these data through curve-fitting of the unanodized and uninterpolated spectral digits. For this, differences between the observed and synthetic spectra were minimized by iterating simultaneously the position and intensity of each spectral feature⁷. **Figure 2** illustrates the method for lines near $4900.8\ \text{cm}^{-1}$ in one of the cold temperature scans; a Voigt line shape and a sine instrument function were used for the computed trace. Very weak features and the residual water lines were fitted to obtain the proper continuum values, but the water features and lines with optical depths less than 5% or greater than 90% were later excluded from consideration. Over 14000 individual measurements were retrieved from 16 room temperature spectra. These were combined so that the position and intensity of each feature could be determined as an average of up to 12 different scans. Known transition assignments and ground state energies were matched to the measurements so that individual intensities could be normalized to 296 K before averaging. For the unidentified lines and the $^{15}\text{NH}_3$ transitions, the resulting intensities were determined at 294 K (see **Table 1**). The data from the 6 m white cell revealed that there was an enriched residual $^{15}\text{NH}_3$ present, and so these data were not utilized for the isotopic intensities.

The measured line centers of the 2.0 band of CO were compared to the values of

Pollock et al.⁸ to establish a frequency calibration using multiplying factors applied to the retrieved line positions of each ammonia spectrum. The line centers of H₂O between 5206 and 5396 cm⁻¹ were also calibrated against the CO lines so that the all ammonia data could be normalized to the same standard. **Table 2** lists the resulting H₂O positions in cm⁻¹ along with the rms agreement (based on three different spectra) and the quantum assignment. The last column shows the differences between the observed and 111 TRAN⁵ positions (o-c); the average difference is -0.0023 cm⁻¹. Typically, the rms agreement with the standards after the correction factor had been applied was 0.00003 cm⁻¹ with CO and 0.00005 with H₂O. However, the absolute accuracies of the NH₃ lines were somewhat worse because of the density of overlapping lines and because of pressure shifts associated with self-broadening. The recent Raynaud et al. study⁹ “of 11 transitions of ν_2 near 900 cm⁻¹ reported that shifts were both negative and positive and varied from 0.66 to 3.77 Mhz/Torr. If pressure shifts increase proportionally with frequency, then the shift for NH₃ lines at 2 μ m could be a factor of 5 larger (or from 0.0001 to 0.0005 cm⁻¹ error).

Tables 3 and 4 give examples of the experimental results. The upper part of **Table 3** lists the individual room temperature measurements at different paths and pressures that were retrieved for the ^PP₁(4) s transition of ν_3 -t ν_4 . The averaged values are listed at the bottom of each part along with the computed rms of the differences between each observed and averaged value (ob-av for positions and Diff% for intensities). The rms values are taken as an indication of experimental precision or uncertainties. **Table 4** lists the measurements for 39 randomly-selected transitions, The experimental uncertainties for each quantity (shown in parentheses) have been computed as the rms differences between the

10- 20%.

As with methane¹⁰ and ammonia at 5 μm ¹¹, the lower state transition energies of the N] I_3 lines were obtained experimentally by measuring line intensities at different temperatures (T_1, T_2) and solving for E'' in Eq. 1

$$\frac{\text{Int (at } T_1)}{\text{Int (at } T_2)} = \frac{Q_2 \exp(-1.4388E''/T_1) (1 - \exp(-1.4388\nu / T_1))^{-n}}{Q_1 \exp(-1.4388E''/T_2) (1 - \exp(-1.4388\nu / T_2))^{-n}} \quad \text{Eq. 1}$$

where Q is the total partition function evaluated at each temperature. Cold sample data shown in Table 1 were measured to produce over 16000 individual retrievals. The lower part of Table 3 gives empirical lower states for $\text{P}_1(4)$ s of $\nu_3 + \nu_4$. Here the individual intensities at low temperatures were combined with the averaged room temperature intensity (from the upper part of the table) to obtain an averaged empirical lower state. The "Diff" columns show the (observed - averaged) / average in percent. The label "r" indicates that the deviate values were rejected from the averaged lower state. The rms agreement is 22.2% indicating a high uncertainty for this lower state, but empirical energy is still within 1.8% of the value expected from the assignment. To validate the lower state energies, the empirical values were compared to calculated ground states¹¹ for some of the stronger assigned lines^{2,4}. Table 4 also gives a sample of lower state energies with the percent differences between the observed value and the calculated ground state shown in the far right column. Transitions with lower states of less than 250 cm^{-1} are expected to have worse experimental uncertainties¹⁰. The good agreement seen in Table 4 is an indication

averaged and individual measurements. As seen there, the rms values for positions range from 0.00001 to 0.00067 cm^{-1} . The precision of the unblended lines are often 0.0003 cm^{-1} or better, but because of possible pressure shifts, absolute accuracy of the NH_3 positions is set conservatively to 0.0007 cm^{-1} for unblended lines. For blended features, the absolute accuracy degrades to 0.003 cm^{-1} .

Achieving a good absolute accuracy for the intensities proved difficult because of ammonia adsorption to the cell walls. Intensity measurements from different sets of data were systematically different by 4 to 16% with the largest deviations occurring for runs done with the 6 m white cell. To compensate for this problem with the gas sample, additional scans were taken, and each optical density was normalized to make its intensities fall close to the mean average determined from the intensities of a few hundred transitions with known assignments. This approach hopefully produced consistent precisions for all the well-isolated features in the spectra. **Tables 3** and 4 provide some validation of this point in that the rms values for intensities (uric%) fall in the range of 1. to 3.5% for intensities. The quality of the intensities can also be judged by comparing pairs of lines with the same rotational quantum numbers which arise from the a and s inversion levels. In unperturbed bands, these pairs are expected to have similar intensities within a few percent, and this is the case for most of the pairs shown. The transition pairs in **Table 4** are typical of the agreement seen for isolated lines. The precision of the intensities for unblended lines appears to be $\pm 3\%$ or better through all three orders of magnitude of intensity. The absolute accuracy of the data is set conservatively to $\pm 7\%$ because the systematics may not have been properly corrected. The accuracy of the blended intensities is in the range of

that the normalization of the optical densities has resulted in good consistency. It should be noted, however, that the uncertainties for the unassigned lines will be worse because the room temperature intensity has not been normalized to 296 K before computing the average. In addition, the weakest features are based on only two or three spectra, rather than the 10 -12 runs available for the strongest lines.

RESULTS and DISCUSSION

In all, line positions and intensities of 2000 NH_3 features with intensity greater than $3.0 \times 10^{-24} \text{ cm}^{-1} / (\text{molecule-cm}^{-2})$ at room temperature were measured, and the lower state energies were determined for 1815 of these. The resulting linelist was validated by comparing observed spectrum to a synthetic spectrum calculated from the averaged values. For example, a 10 cm^{-1} portion of the observed apodized spectrum in the region of ${}^R\text{Q}_0$ of $\nu_3 + \nu_4$ is shown in Figure 3.

An intermediate version of the empirical lower states and the method of combination differences permitted the identification of additional transitions. Since a composite calculation from quantum mechanics was not available, assignments were pursued for only the allowed transitions of perpendicular bands: $\Delta J = \pm 1$ and O, $\Delta K = \pm 1$ with $\Delta l = \pm 1$, and $s \leftrightarrow s$, $a \leftrightarrow a$. For the main isotope of $\nu_3 + \nu_4$, very few corrections of the Sarangi identifications were required other than interpreting features that were unresolved blends in his low resolution data. Portions of the $\nu_3 + \nu_4$ band of ${}^{15}\text{NH}_3$ were then assigned readily by inspection of the spectrum obtained with the enriched sample; the assignments included

in the 1996 HITRAN database are shown in **Table 5**. For $\nu_1 + \nu_4$, the 119 assignments of Coy and Lehmann provided an excellent starting point (although it was found that their line centers were low by 0.004 cm⁻¹), and the number of identified transitions were doubled by following sub-bands up to $J = 10$. Upper states were determined for both bands by adding the transition frequencies to the computed lower state¹² to obtain an averaged upper state value. The **Table 6** lists the experimental upper states for $\nu_1 + \nu_4$ with results of the present study labelled as "N." The rms difference [when n transitions to the same upper state are used] is computed and can be used to estimate the precision of the measured positions. **Table 6** and a similar list for $\nu_3 + \nu_4$ can be obtained electronically to facilitate theoretical studies of these bands and hot bands in other regions. It should be expected that a good theoretical modeling of the data will reveal some incorrect assignments. With 55% of the lines being unidentified, there are probably some matches to combination differences that are purely coincidental. The most suspect levels are those based on only one assignment. For example, the RQ_0 lines of both bands have been located, but it is likely that some of the J values are incorrectly ascribed.

The empirical values for the band centers in cm⁻¹ were determined from the $J',K' = 0,0$ levels by adding the computed ground state to the observed line positions of the $^P(1,1)$ transitions. As shown in **Table 7**, the isotopic shift for $\nu_3 + \nu_4$ is 11.37 cm⁻¹.

The positions, intensities and lower state energies were written into HITRAN database format. Whenever an assignment was known, the empirical ground state was replaced by the corresponding calculated value rounded to the nearest 0.1 cm⁻¹. For the unassigned lines, the rms of empirical lower state was divided by 100 and added to the

lower state value in order to retain the experimental uncertainty in the database. For example, the line at 4940.1703 cm^{-1} listed with E'' of 527.0312 cm^{-1} should be interpreted as $E'' = 527.0 \pm 3.12\%$. The intensities for $^{15}\text{NH}_3$ were scaled by the isotopic abundance of 0.0035. **Table 8** gives a summary of the experimental parameters. The lower portion shows the number of total lines, range of positions, number of isotopes, vibrational states, bands and the total integrated intensity computed by summing the observed intensities. The upper portion gives similar information by band including the range of intensities and the sum of the intensities for assigned lines. The strongest unassigned line has an intensity of 3.6×10^{-21} . The fact that the intensity sum of all the unassigned lines is only 13% of the total intensity of the region indicates that the dominant structure of the region is now well-characterized.

The intensity summations in **Table 8** represent reasonable lower limits for integrated intensities of the two combination bands. To provide a perspective of ammonia band intensities, the $2\text{ }\mu\text{m}$ values are listed in Table 9 with the results for bands at 4, 3 and $2.3\text{ }\mu\text{m}$. The band strengths (S_v) obtained by fitting measurements to hamiltonian models are listed in the third column while summations of individual line intensities are shown in the fourth column. The underlined values are the result of combining the strengths for the a and s inversion states. The total $\nu_3 + \nu_4$ absorption of $15.66\text{ cm}^{-2}\cdot\text{atm}^{-1}$ at 296 K (obtained from 537 assignments) is similar to Sarangi's value of $17.19\text{ cm}^{-2}\cdot\text{atm}^{-1}$ at 296 K obtained by fitting 291 intensities.³ The other band strengths¹³⁻¹⁵ were obtained by modeling selected intensities. The values for the four states near 2400 cm^{-1} were reported by Kleiner et al.¹³ who used 700 intensities (retrieved from some of the same Kitt Peak spectra used in the present effort). The intensities of nearly 300 other transitions were also measured, and

their integrated sum is listed as “unassigned” (these are mainly hot band lines). For two fundamentals near 3400 cm^{-1} , Pine and Dang-Nhu modeled 91 intensities of ν_1 and ν_3 .¹⁴ The two combination bands near 4400 cm^{-1} were reported by Margolis and Kwan who fitted 220 lines of $\nu_1 + \nu_2$ and $\nu_2 + \nu_3$.¹⁵ The last two studies used isolated-band models, but all studies noted that a portion of their available data could not be reproduced within experimental uncertainties. The successful modeling of the $3\text{--}2\text{ }\mu\text{m}$ intensities is expected to be very challenging.

In 1977, Sarangi measured 2100 lines at $2\text{ }\mu\text{m}$ and assigned 27% of them. It is now seen that features belonging to $\nu_1 + \nu_4$ were among his unidentified lines. In the present study, a similar set of features was measured with better accuracy and thoroughness, and 45% of the observations were identified. Still, half of the region remains unassigned. Of these unknown lines, 80% have empirical lower states that are less than 930 cm^{-1} , indicating that these features are not hot band transitions. Some of these are surely forbidden ($\Delta K = 3, 5$ or $\Delta l = \pm 2$) transitions of the combination bands. Some forbidden transitions computed using the empirical upper states did match observed positions with an appropriate empirical lower state, but these were not included because there was no intensity calculation available to confirm the probable assignments. Other unassigned lines must be transitions from the A component of $\nu_3 + \nu_4$ which probably lies within 40 cm^{-1} of observed E state. Some transitions must also arise from other vibrational states in the region. It should be expected that their intensities are sometimes enhanced by resonance with one of the strong combination bands. Evidence of interaction is seen in PQ_1 at $J = 4$ of $\nu_3 + \nu_4$ where the intensity is almost half the expected amount, and an extra feature appears. ‘J’ but, it is

thought that the intensities for the a and s inversion pairs of 1P_1 4 and 1P_2 5 in Table 4 are unequal because of resonance with another vibrational level. The most likely perturbing state is $2\nu_2 + \nu_3$ near 5040 cm^{-1} . Clearly, with resonances occurring at the lowest K values, it will be necessary to employ a multi-state model to interpret this region fully.

CONCLUSION

There is now an extensive set of measurements for ammonia at $2\text{ }\mu\text{m}$. All the strong lines in the region are identified, and most of the unassigned features have empirical lower state energies. The theoretical modeling of these data should be pursued. For the interim, the results are organized and available in electronic format (to receive the lists described, contact the first author at linda@regina.jpl.nasa.gov).

ACKNOWLEDGEMENTS

The authors are deeply indebted to Coy and Lehmann who provided their $2\text{ }\mu\text{m}$ results in electronic form. We also thank the Kitt Peak National Observatory/National Solar Observatory for the use of the ITS and C. Plymate and J. Wagner for assistance in obtaining the NH_3 spectra. The research reported in this paper was performed at the Jet Propulsion Laboratory, California Institute of Technology, under contract with the National Aeronautics and Space Administration.

REFERENCES

1. W. S. Benedict and E. K. Plyler, *Canad. J. Phys.* **35**, 1235 (1957).
2. S. Sarangi, *J. Quant. Spectrosc. Radiat. Transfer* **18**, 257 (1977).
3. S. Sarangi, *J. Quant. Spectrosc. Radiat. Transfer* **18**, 289 (1977).
4. S. L. Coy, and K. K. Lehmann, *Spectrochimica Acta* **45**, 47-56 (1989).
5. L. S. Rothman, R. R. Gamache, R. H. Tipping, C. P. Rinsland, M. A. H. Smith, D. Chris Benner, V. Malathy Devi, J.-M. Flaud, C. Camy-Peyret, A. Perrin, A. Goldman, S. T. Massie, L. R. Brown, and R. A. Toth, *J. Quant. Spectrosc. Radiat. Transfer* **48**, 469 (1992).
6. N. I. Iusson, B. Bonnet, N. A. Scott, and A. Chedin, *J. Quant. Spectrosc. Radiat. Transfer* **48**, 509 (1992).
7. L. R. Brown, J. S. Margolis, R. H. Norton, and B. D. Stedry, *Appl. Spectrosc.* **37**, 287 (1983).
8. C. R. Pollock, F. R. Petersen, D. A. Jennings, J. S. Wells, and A. G. Maki, *J. Mol. Spectrosc.* **107**, 62 (1984).
9. F. Raynaud, B. Lemoine, and F. Rohart, *J. Mol. Spectrosc.* **168**, 584 (1994).
10. J. S. Margolis, *Appl. Opt.* **29**, 3426- (1990).
11. E. Lellouch, N. I. Iacome, G. Guelachvili, G. Tarrago, and T. Encernaz, *J. Mol. Spectrosc.* **124**, 333 (1987).
12. R. L. Poynter and J. S. Margolis, *Mol. Phys.* **48**, 401 (1983).
13. I. Kleiner, G. Tarrago, and L. R. Brown, *J. Mol. Spectrosc.* **173**, 120 (1995).
14. A. S. Pine and M. Dang-Nhu, *J. Quant. Spectrosc. Rad. Transfer* **50**, 565 (1993).
15. J. S. Margolis and Y. Y. Kwan, *J. Mol. Spectrosc.* **50**, 266 (1974).

FIGURES

Fig. 1 The spectrum of ammonia at $2\ \mu\text{m}$ ($5000\ \text{cm}^{-1}$) obtained with the FTS at Kitt Peak. The pressure is 1.01 Torr at 294.7 K and the optical path is 1.5 m. The apodized resolution is $0.016\ \text{cm}^{-1}$.

Fig. 2 Measurement of positions and intensities by curve-fitting the unapodized spectrum. The observed and computed spectra are overlaid in the lower frame, and their percent differences are plotted in the upper panel. The vertical lines in between indicate the features that were measured by simultaneously adjusting the calculated positions and intensities. The optical path is 16 m and the pressure is 1.06 Torr at 192 K. The three largest lines are $^R\text{P}_1(7)$ s of $\nu_3 + \nu_4$ at $4900.6912\ \text{cm}^{-1}$ and the two inversion pairs of $^i\text{P}_1(3)$ of $\nu_1 + \nu_4$ at 4900.8396 and $4901.0133\ \text{cm}^{-1}$ respectively.

Fig. 3 Validation of the ammonia positions and intensities by comparing the observed data to a synthetic spectrum based on the retrieved positions and intensities. In the upper frame, the observed and computed spectra are overlaid, and the percent differences are plotted in the lower panel. The optical path is 1.5 m and the pressure is 2.66 Torr at 294.6 K. The strong lines belong to $^R\text{Q}_0$ of $\nu_3 + \nu_4$ starting with $J_0' = 1$ and 2 near $5046\ \text{cm}^{-1}$.

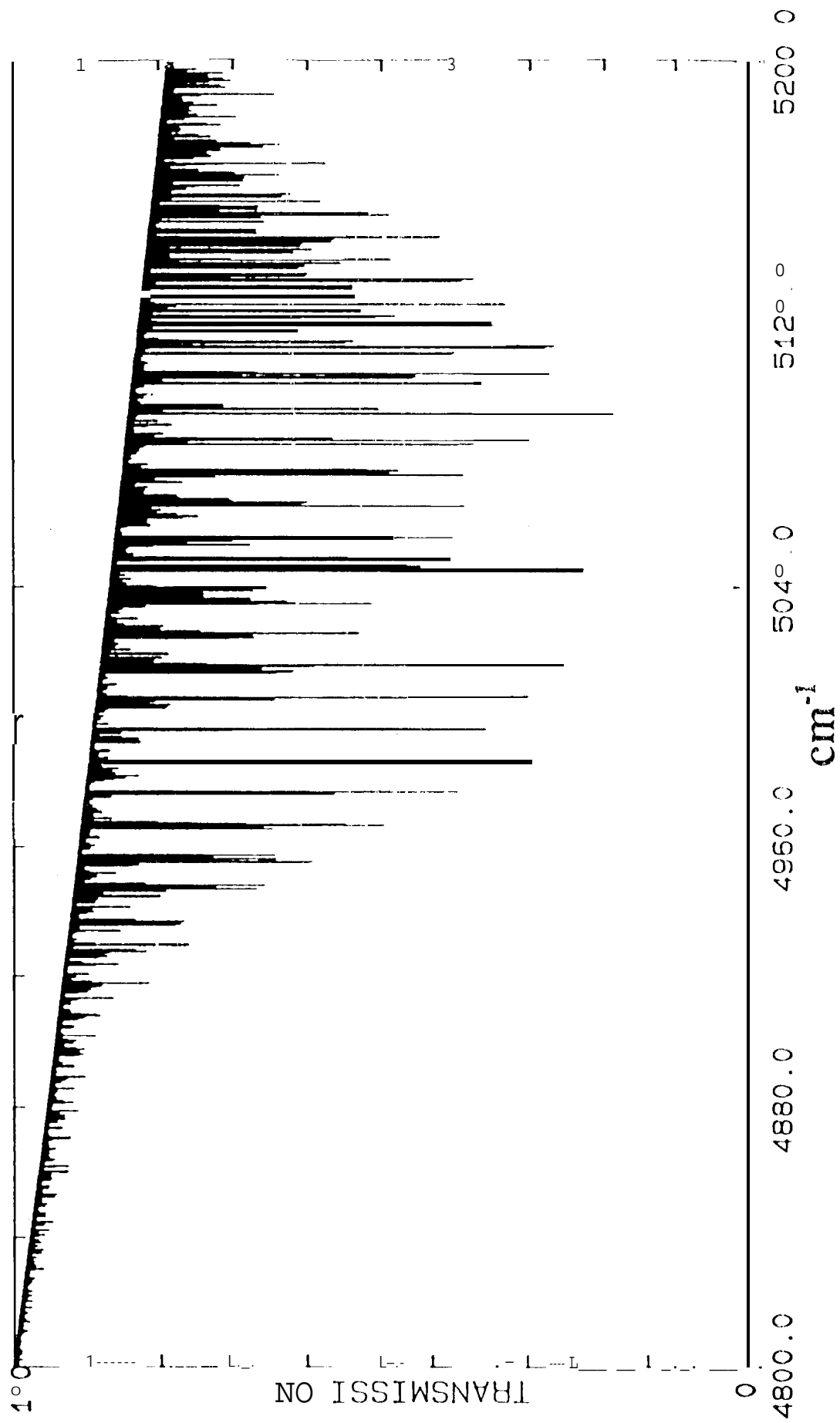


Fig. 1

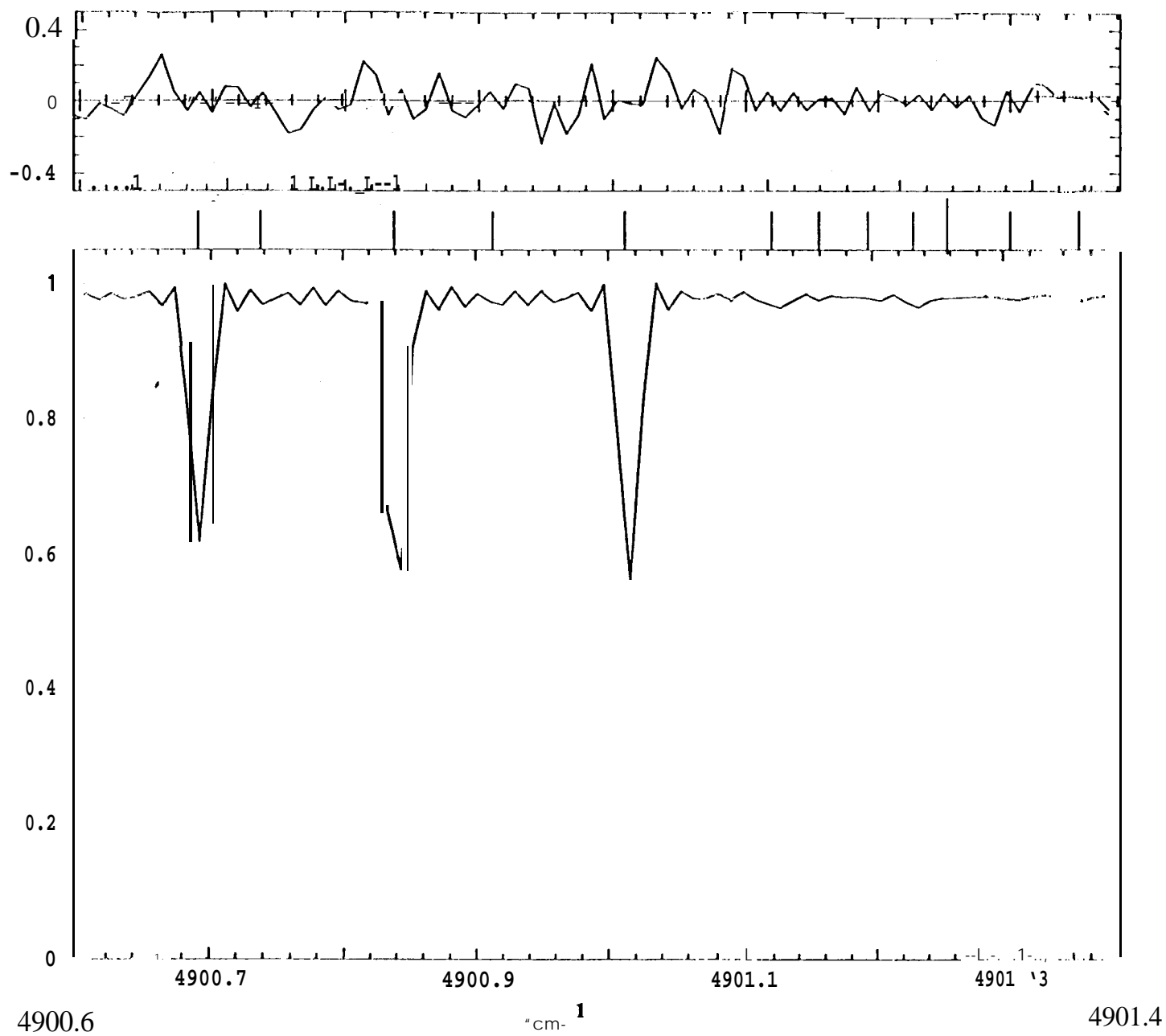


Fig. 2

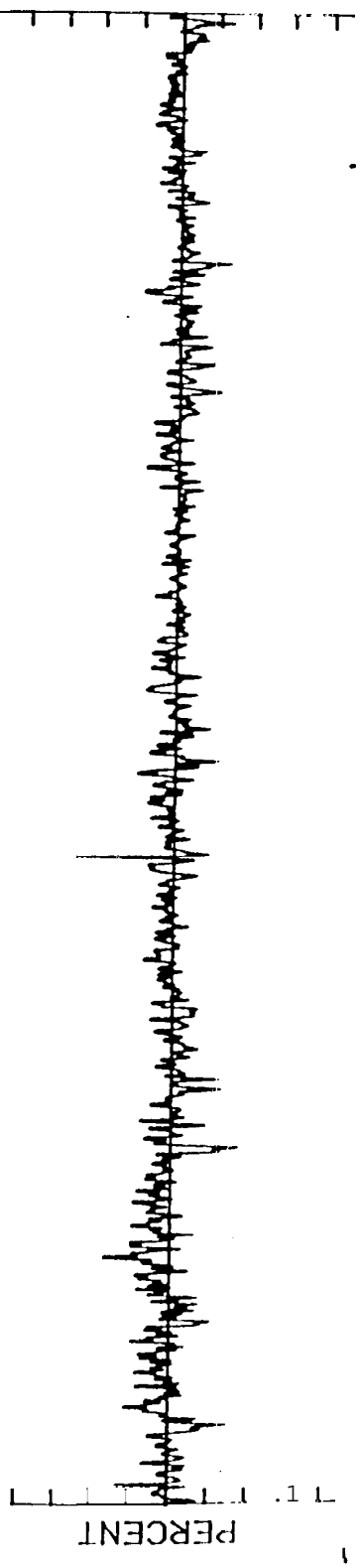
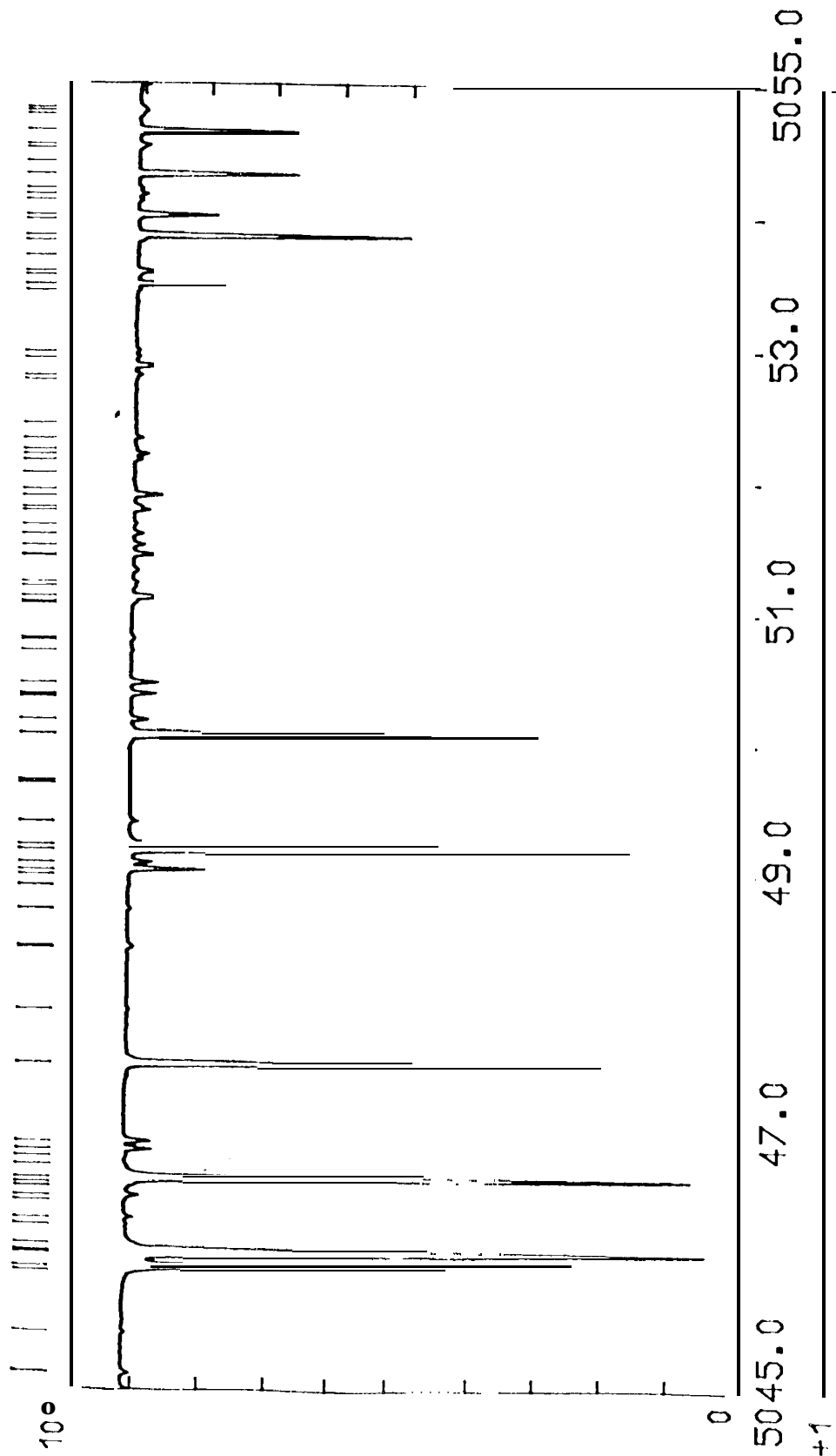


Fig 3

TABLES

Table 1	Summary of Ammonia laboratory Data
Table 2	H ₂ O Line Positions Calibrated by CO
Table 3	Sample of Individual Measurements
Table 4	Sample of Empirical Intensities and Lower State Energies of $\nu_3 + \nu_4$ lines
Table 5	Assignments of the $\nu_3 + \nu_4$ Band of ¹⁵ NH ₃ in the 1996 HITRAN Database
Table 6	Upper state Energies of $\nu_1 + \nu_4$ of ¹⁴ NH ₃
Table 7	Comparison of Ammonia Band Centers in cm ⁻¹
Table 8	Summary of the 1996 HITRAN NH ₃ Parameters at 2 μ m
Table 9	Summary of NH ₃ Intensity Measurements in Four Regions

ROOM TEMPERATURE				COLD TEMPERATURE			
MOLECULE	PRES Torr	PATH m	TEMP K	MOLECULE	PRES Torr	PATH m	TEMP K
NH3-14	* 1.07	0.25	291.5	NH3-14	0.99	0.80	189.0
NH3-14	3.50	0.25	298.7	NH3-14	1.99	0.80	190.0
NH3-14	* 2.84	0.25	290.7	NH3-14	1.97	0.80	189.0
NH3-14	1.01	1.50	294.7	NH3-14	1.03	0.80	233.0
NH3-14	2.66	1.50	294.6	NH3-14	1.96	0.80	240.0
NH3-14	5.42	0.25	295.8				
NH3-14	8.51	0.25	295.8	NH3-14	20.00	0.80	220.0
NH3-14	30.05	0.25	295.8	NH3	1*77	4.33	185.0
NH3-14	0.50	0.80	293.6	NH3	1.77	4.33	195.
NH3-14	1.01	0.80	294.0	NH3	0.78	4.33	215.0
NH3-14	2.01	0.80	296.0	NH3	1.77	4.33	220.0
NH3-14	0.90	0.25	293.8	NH3	1.06	16.41	192.0
NH3-14	* 0.51	0.25	289.7	NH 3	2.03	16.41	200.0
NH3	0.52	25.0	295.5	NH3	1.47	24.41	211.0
NH3-15	2.02	0.25	293.8				
NH3-15	0.90	0.25	293.8				

[†] NH3-14 and NH3-15 are 99.9% and 99.0% enriched samples of N¹⁴ and N¹⁵, respectively. The runs with * contained CO in the 0.25 m cell and were used to calibrate H₂O line positions near 5300 cm⁻¹. The average temperature of the room temperature data is 294.3 ± 2.3 K.

Table 2 H₂O LINE POSITIONS CALIBRATED BY CO

obs cm-l	unc	Band	J'	K'	K'	J''	K''	K''	o-c cm-l
5206.31133	(4)	011	5	1	5	6	1	6	-0.0027
5206.51541	(4)	011	4	2	2	5	2	3	-0.0026
5208.82798	(7)	011	4	1	3	5	1	4	-0.0010
5225.32334	(9)	011	4	0	4	5	0	5	-0.0017
5243.88629	(2)	011	3	2	2	4	2	3	-0.0027
5244.58143	(7)	011	3	0	3	4	0	4	-0.0026
5248.30602	(9)	011	3	1	3	4	1	4	-0.0020
5254.80604	(4)	011	2	1	1	3	1	2	-0.0030
5261.49974	(3)	011	2	2	0	3	2	1	-0.0013
5263.97506	(3)	011	2	0	2	3	0	3	-0.0029
5269.13261	(3)	011	2	1	2	3	1	3	-0.0034
5284.78010	(3)	011	1	0	1	2	0	2	-0.0019
5290.26571	(3)	011	1	1	1	2	1	2	-0.0023
5307.47286	(4)	011	0	0	0	1	0	1	-0.0021
5327.39037	(5)	011	1	1	1	1	1	0	-0.0016
5332.09221	(4)	011	3	2	2	3	2	1	-0.0028
5336.18694	(8)	011	2	2	1	2	2	0	-0.0021
5338.22622	(3)	011	1	1	0	1	1	1	-0.0018
5338.75447	(3)	011	2	2	0	2	2	1	-0.0005
5344.52450	(8)	011	3	3	1	3	3	0	-0.0015
5344.92315	(7)	011	3	3	0	3	3	1	-0.0028
5345.05382	(8)	011	4	3	1	4	3	2	-0.0032
5348.67552	(3).	011	2	1	1	2	1	2	-0.0025
5374.27402	(4)	011	2	1	2	1	1	1	-0.0030
5376.94239	(4)	011	2	0	2	1	0	1	-0.0026
5385.80013	(3)	011	2	1	1	1	1	0	-0.0029
5393.64808	(3)	011	3	1	3	2	1	2	-0.0019
5396.54341	(9)	011	3	0	3	2	0	2	-0.0026

The average observed - HITRAN (o-c) is -0.0023 cm⁻¹.

Table 3

SAMPLE OF INDIVIDUAL MEASUREMENTS

" Room Temperature Results*

Positions cm ⁻¹	Obs-av cm ⁻¹	Intensity cm ⁻² /atm ⁻¹	Diff %	Temp K	Path m	Pres Torr
4977.017076	-0.00014	1.817E-02	-1.6	290.7	10.25	2.840
4977.017140	-0.00008	1.836E-02	-0.6	295.8	0.25	5.420
4977.017155	-0.00006	1.864E-02	0.9	295.8	0.25	10.050
4977.017186	-0.00003	1.880E-02	1.8	294.0	1.50	1.010
4977.017200	-0.00002	1.893E-02	2.5	294.6	1.50	2.660
4977.017213	0.00000	1.900E-02	2.9	296.0	25.00	0.520
4977.017270	0.00005	1.763E-02	-4.6	289.7	0.25	0.513
4977.037300	0.00008	1.881E-02	1.8	294.0	0.80	1.010
4977.017340	0.00012	1.782E-02	-3.5	295.8	0.25	8.510
4977.017387	0.00017	1.878E-02	1.7	293.6	0.80	0.504
4977.017215	0.00009	1.847E-02	1.7	= averaged values		

Cold Temperature Results

Intensity at Temp	E" (ith)	Diff %	Temp K	Path m	Pres Torr
2.286E-02	329.77 r	66.2	185.0	4.33	1.770
3.684E-02	156.66	-21.0	189.0	0.80	1.974
3.535E-02	171.66,	-13.4	189.0	0.80	0.994
3.493E-02	173.74	-12.4	190.0	0.80	1.990
2.957E-02	232.27	17.0	192.0	16.41	1.068
2.317E-02	324.39 r	63.5	195.0	4.33	1.770
2.546E-02	282.51	42.3	200.0	16.41	2.030
2.749E-02	229.14	15.4	211.0	24.41	1.470
2.853E-02	186.31	-6.0	219.0	0.80	2.028
2.360E-02	295.82 r	49.1	220.0	4.33	1.770
2.577E-02	243.44	22.7	220.0	0.80	20.000
2.828E-02	131.10	-33.9	233.0	0.80	1.029
2.552E-02	177.21	-10.6	240.0	0.80	1.956

E" empirical = 198.0 (22.2) E" calculated = 194.9000

* E" is the lower state energy in cm⁻¹.

Table 4 Sample of Empirical Intensities and Lower State Energies of v_3+v_4 Lines[†]

Observed Position	Unc	Observed Intensity	Unc (%)	l	J'	K'	J''	K''	Observed E''	Unc (%)	E'' %0-c
4986.69604	(11)	2.86E-21	(2.5)	1	2	1	3	0 s	111.7	(11.3)	-6.7
4967.13578	(4)	2.75E-21	(1.8)	1	3	1	4	0 a	199.6	(14.5)	0.1
4948.79747	(9)	1.99E-21	(1.2)	1	4	1	5	0 s	307.0	(9.9)	3.1
4930.29499	(7)	1.18E-21	(1.6)	1	5	1	6	0a	419.9	(3.8)	0.7
4913.86267	(17)	4.67E-22	(2.5)	1	6	1	7	0 s	560.0	(3.9)	1.0
4976.67274	(21)	1.10E-21	(1.7)	-1	3	0	4	1a	216.1	(18.4)	9.5
4977.01722	(9)	7.46E-22	(1.7)	-1	3	0	4	1s	198.0	(22.2)	1.8
4967.83907	(16)	1.13E-21	(2.2)	-1	4	1	5	2a	287.1	(10.1)	1.2
4968.15326	(2)	5.08E-22	(3.5)	-1	4	1	5	2 s	296.3	(11.8)	4.5
4936.41442	(15)	4.40E-22	(1.2)	-1	5	0	6	3a	431.7	(4.0)	4.8
4936.66990	(6)	4.40E-22	(1.2)	-1	5	0	6	1 s	425.4	(5.4)	3.0
4967.48947	(01)	1.75E-21	(1.5)	-1	5	3	6	4a	355.0	(4.9)	-0.9
4967.78507	(10)	1.73E-21	(2.0)	-1	5	3	6	4s	356.6	(5.1)	-0.9
4977.26352	(23)	2.58E-21	(3.2)	-1	5	4	6	5a	307.7	(18.8)	-5.7
4977.55102	(17)	2.58E-21	(1.0)	-1	5	4	6	5s	322.7	(7.3)	-0.9
4957.63019	(11)	1.33E-21	(2.5)	-1	6	4	7	5a	466.8	(3.0)	0.7
4957.94747	(16)	1.35E-21	(2.2)	-1	6	4	7	5s	455.0	(4.4)	-1.1
4967.22658	(12)	3.94E-21	(1.4)	-1	6	5	7	6a	439.7	(8.5)	3.4
4967.57292	(16)	3.19E-21	(1.4)	-1	6	5	7	6s	416.2	(5.1)	-1.1
4993.01400	(23)	4.64E-22	(3.5)	1	6	6	6	5 a	335.8	(7.8)	3.7
4993.33097	(55)	4.52E-22	(2.7)	1	6	6	6	5 s	332.9	(8.1)	2.9
4976.52439	(22)	2.98E-21	(2.0)	-1	6	6	7	7a	369.2	(4.9)	-1.0
4976.78238	(30)	3.02E-21	(1.1)	-1	6	6	7	7s	377.2	(5.6)	0.8
4937.91656	(28)	6.25E-22	(3.3)	-1	7	4	8	5a	625.4	(4.1)	0.0
4938.28523	(25)	6.13E-22	(2.5)	-1	7	4	8	5s	627.6	(3.9)	1.0
4947.67365	(12)	1.80E-21	(2.6)	-1	7	5	8	6a	572.4	(6.1)	-1.0
4948.15531	(18)	1.46E-21	(1.7)	-1	7	5	8	6s	581.5	(4.8)	0.0
4928.03340	(20)	7.62E-22	(2.2)	-1	8	5	9	6a	758.5	(6.2)	-0.9
4928.56618	(33)	6.53E-22	(2.0)	-1	8	5	9	6s	741.8	(5.6)	-2.9
4946.86893	(14)	8.75E-22	(3.6)	-1	8	7	9	8a	652.0	(7.6)	-0.9
4947.19793	(23)	8.83E-22	(1.4)	-1	8	7	9	8s	655.5	(5.3)	0.0
4955.76155	(21)	2.74E-21	(2.3)	-1	8	8	9	9a	583.7	(5.9)	-1.7
4956.05587	(31)	2.78E-21	(2.0)	-1	8	8	9	9s	572.9	(9.1)	-3.4
4936.55905	(20)	1.04E-21	(1.1)	-1	9	8	10	9 a	790.6	(6.3)	-0.9
4936.91757	(29)	1.04E-21	(1.1)	-1	9	8	10	9 s	786.3	(7.1)	-0.9
4945.23130	(26)	8.47E-22	(2.0)	-1	9	9	10	10 a	707.7	(4.5)	-1.0
4945.52892	(32)	8.51E-22	(2.6)	-1	9	9	10	10 s	708.6	(4.3)	-1.0
4934.61230	(41)	4.72E-22	(2.0)	-1	10	10	11	11 a	854.3	(8.1)	-4.0
4934.90616	(67)	4.84E-22	(2.0)	-1	10	10	11	11 s	854.3	(9.1)	-3.0

[†] Positions and lower state energies E'' are given in units of cm⁻¹, and the intensities are in units of cm⁻¹/(molecule·cm⁻²) near 296 K. The experimental uncertainties are the computed rms values based on the measurements. For positions, the uncertainties in the last 2 digits are indicated. For intensities and lower state energies, the uncertainties are given in percent.

Table 5 Assignments of the $\nu_3+\nu_4$ Band of $^{15}\text{NH}_3$ in the 1996 HITRAN Database

Position	Intensity	J'K'l	J''K''l	Position	Intensity	J'K'l	J''K''l	Position	Intensity	J'K'l	J''K''l
4944.49918	75E-24	8 8 -1 a	9 9 0 a	5015.2866	3.05E-24	63 1 a	6 20 a	5091.8322	1.81E-23	5 5 1 s	4 4 0 s
4944.49918	75E-24	8 8 -1 s	9 9 0 s	5015.4276	1.03E-23	11 -1 s	2 20 s	5093.2051	1.22E-23	43 1 a	32 0 a
4945.7196	7.34E-24	5 2 -1 a	63 0 a	5024.1708	5.24E-24	22 1 a	2 10 a	5093.5088	1.27E-23	4 3 1 s	3 2 0 s
4946.7470	4.39E-24	76 -1 s	870 s	5024.3549	1.21E-23	22 1 s	2 10 s	5094.3150	3.74E-24	75 -1 a	76 0 a
4946.4055	4.33E-24	64 -1 a	75 0 a	5024.6764	6.85E-24	3 2 1 s	3 10 s	5094.3859	2.27E-23	3 11 a	200 a
4946.5735	3.40E-24	64 -1 s	75 0 s	5024.7515	6.25E-24	4 2 1 a	4 10 a	5094.4509	4.07E-24	75 -1 s	7 6 0 s
4955.1618	6.73E-24	7 7 -1 s	8 8 0 s	5025.0724	4.02E-24	0 0 -1 s	1 10 s	5094.7232	4.04E-24	6 5 -1 a	66 0 a
4965.2423	9.59E-24	6 6 -1 a	7 7 0 a	5025.1215	6.38E-24	4 2 1 s	4 10 s	5094.7957	4.15E-24	6 5 -1 s	6 6 0 s
4965.4735	9.55E-24	6 6 -1 s	7 7 0 s	5025.4552	4.75E-24	5 2 1 a	5 10 a	5100.5276	1.53E-23	6 6 1 a	5 5 0 a
4966.0056	2.08E-23	4 2 -1 s	5 3 0 s	5026.0060	4.92E-24	5 2 1 s	5 10 s	5100.9223	1.54E-23	66 1 s	5 5 0 s
4966.1499	1.29E-23	4 2 -1 a	5 3 0 a	5027.4533	3.12E-24	6 2 1 s	6 10 s	5102.4361	2.50E-23	5 4 1 a	4 3 0 a
4966.2333	7.94E-24	5 4 -1 s	6 5 0 s	50%5.5849	3.07E-23	111 s	1 00 s	5102.8422	2.54E-23	54 1 s	43 0 s
4975.4416	9.31E-24	2 1 1 s	3 0 0 s	5034.6769	2.28E-23	2 1 1 a	2 00 a	5103.8909	4.35E-23	4 2 1 a	3 10 a
4975.4572	2.47E-23	5 5 -1 a	660 a	5035.2434	3.15E-23	3 1 1 s	3 00 s	5104.2963	2.72E-22	4 2 1 s	3 10 s
4975.6764	2.47E-23	5 5 -1 s	660 s	5035.6346	2.44E-23	4 11 a	4 00 a	5109.5615	2.42E-23	77 1 s	66 0 s
4975.9244	1.28E-23	3 1 -1 a	4 2 0 a	5037.6774	1.63E-23	5 1 1 s	5 00 s	5111.5133	1.08E-23	65 1 a	5 4 0 a
4976.1683	9.72E-24	3 1 -1 s	4 2 0 s	5038.7249	8.99E-24	6 1 1 a	6 00 a	5112.0940	1.11E-23	6 5 1 s	5 4 0 s
4985.3563	1.74E-23	2 0 -? a	3 1 C a	5042.3289	4.88E-24	7 1 1 s	7 00 s	5113.2963	9.07E-24	5 3 1 a	4 2 0 a
4985.5648	1.40E-23	4 4 -? a	5 5 0 a	5044.0873	1.91E-23	5 0 -1 s	5 10 s	5113.7905	8.99E-24	5 3 1 a	4 2 0 s
4985.7682	1.46E-23	4 4 -1 s	5 5 0 s	5044.4040	5.68E-24	4 0 -1 a	4 10 a	5115.5400	1.98E-23	4 11 s	3 0 0 s
4986.0060	1.99E-23	3 2 -1 s	4 3 0 s	5044.4682	6.73E-24	4 0 -1 s	4 10 s	5117.9106	8.55E-24	88 1 a	770 a
4994.8803	6.17E-24	2 0 -1 a	3 1 0 a	5044.7808	1.11E-23	2 0 -1 a	2 10 a	5118.4744	9.15E-24	88 1 s	77 0 s
4995.5639	2.38E-23	3 2 -1 a	4 3 0 a	5044.8002	6.05E-24	1 0 -1 a	1 10 a	5120.6947	8.30E-24	76 1 a	65 0 a
4995.7578	1.56E-23	3 2 -1 a	4 3 0 a	5045.0347	7.54E-24	2 0 -1 s	2 10 s	5121.4763	8.22E-24	76 1 s	65 0 s
4995.7750	8.38E-24	4 4 -1 s	5 5 0 s	5054.3551	1.65E-23	1 1 1 a	0 00 a	5122.6142	1.60E-23	64 1 a	5 3 0 a
5003.7728	6.33E-24	4 4 1 a	4 3 0 a	5055.0141	5.68E-24	2 1 -1 a	2 20 a	5123.2069	1.61E-23	64 1 s	5 3 0 s
5003.3991	6.33E-24	4 4 1 s	4 3 0 s	5055.0960	3.27E-24	3 1 -1 a	3 20 a	5124.2310	6.13E-24	5 2 1 a	4 10 a
5003.5396	7.09E-24	5 4 1 a	5 3 0 a	5055.2549	9.39E-24	2 ? -? s	2 0 s	5124.8237	6.34E-24	5 2 1 s	4 10 s
5003.9002	7.21E-24	5 4 1 s	5 3 0 s	5063.8199	1.14E-23	2 2 1 a	1 10 a	5126.4118	5.94E-24	9 9 1 a	8 8 0 a
5004.1547	5.44E-24	64 1 a	63 0 a	5064.0257	1.14E-23	2 2 1 s	1 10 s	5127.1408	6.17E-24	9 9 1 s	88 0 s
5004.6980	5.64E-24	64 1 s	63 0 s	5064.9501	1.15E-23	4 2 -1 s	4 30 s	5128.7120	1.12E-23	8 7 1 a	76 0 a
5005.1513	4.75E-24	1 0 -1 a	2 10 a	5065.0464	1.19E-23	4 2 -1 a	4 30 a	5129.5743	1.15E-23	87 1 s	760 s
5005.2943	3.2X-24	74 1 a	7 3 0 a	5065.2778	9.84E-24	3 2 -1 a	3 30 e	5131.7473	6.09E-24	7 5 1 a	6 4 0 a
5005.3296	4.80E-24	1 0 -1 s	2 10 s	5065.2812	9.96E-24	3 2 -1 s	330 s	5132.6167	6.23E-24	75 1 s	64 0 s
5005.4680	2.83E-23	2 2 -1 a	330 a	5073.1762	1.60E-23	33 1 a	2 20 a	5133.6555	5.64E-24	63 1 a	5 2 0 a
5005.6199	2.84E-23	2 2 -1 s	330 s	5073.4077	1.63E-23	33 1 s	2 20 s	5134.3525	5.84E-24	63 ? s	5 2 0 s
5005.9209	3.52E-24	74 1 s	730 s	5074.5462	2.27E-23	2 11 s	100 s	5135.6975	7.70E-24	1010 1 s	99 0 s
5013.9269	4.23E-24	3 3 1 s	3 20 s	5082.4095	3.63E-23	4 4 1 a	3 30 a	5136.1765	1.39E-23	5 1 1 a	4 00 a
5014.0295	4.96E-24	4 3 1 a	4 20 a	5082.6742	3.68E-23	4 4 1 s	3 30 s	5137.5208	3.98E-24	9 8 1 a	8 7 0 a
5014.2966	5.16E-24	4 3 1 s	4 20 s	5083.7770	1.02E-23	3 2 1 a	2 10 a	5143.1989	7.86E-24	74 1 a	63 0 a
5014.4776	1.9E-21	5 3 1 a	5 20 a	5084.0684	1.05E-23	3 2 1 s	2 10 s	5143.8819	9.07E-24	74 1 s	63 0 s
5014.9261	4.31E-24	5 3 1 s	5 20 s	50%8734	6.85E-22	5 4 -1 a	5 50 a	5158.7121	8.87E-24	6 1 1 s	5 00 s
5015.2482	1.02E-23	1 1 -1 a	2 20 a	5091.5287	1.77E-23	5 5 1 a	4 40 a	5179.7856	4.96E-24	7 1 1 a	60 0 a

* The observed positions and intensities are in units of cm^{-1} and $\text{cm}^{-1}/(\text{molecule}\cdot\text{cm}^{-2})$ respectively.

Table 6

Upper State Energies of v_1+v_4 of $^{14}\text{NH}_3$

J'	K'	sym	E' cm-1	rms	n		E' cm ⁻¹	rms	n	
			l = + 1				l = -1			
0	0	a					4956.91218	(000)	1	
0	0	s					4955.75555	(000)	1	
1	0	a					4977.02662	(009)	2	
1	0	s					4975.94548	(018)	2	
1	1	a	4976.39045	(014)	3		4970.07278	(000)	1	
1	1	s	4974.67580	(000)	1		4968.92675	(000)	1	
2	0	a					5017.29051	(016)	3	
2	0	s					5016.37549	(027)	3	
2	1	a	5015.51128	(031)	3	N	5010.26758	(084)	5	
2	1	s	5016.37710	(005)	2		5009.29096	(012)	2	
2	2	a	5007.50609	(062)	3		4995.47152	(000)	1	
2	2	s	5006.42340	(006)	3		4994.32943	(000)	1	
3	0	a					5077.77697	(020)	3	
3	0	s					5077.14125	(033)	3	
3	1	a	5078.35456	(009)	3		5070.59612	(023)	3	N
3	1	s	5073.90279	(000)	1	N	5069.88465	(022)	2	N
3	2	a	5067.67251	(050)	3		5055.68690	(033)	2	
3	2	s	5066.69921	(076)	3		5054.85879	(006)	2	
3	3	a	5051.16496	(000)	2		5033.09997	(000)	1	
3	3	s	5050.10603	(045)	3		5031.96209	(000)	1	
4	0	a					5158.58181	(025)	3	
4	0	s					5158.34669	(005)	2	
4	1	a	5154.23155	(000)	1		5151.11380	(013)	3	
4	1	s	5159.82744	(001)	2		5150.76521	(071)	3	
4	2	a	5147.62413	(027)	3		5136.04920	(031)	2	
4	2	s	5146.73159	(030)	2		5135.57655	(026)	3	
4	3	a	5131.44021	(069)	2		5113.26748	(016)	2	
4	3	s	5130.53567	(088)	3		5112.63242	(017)	2	
4	4	a	5107.03211	(010)	3		5082.95520	(000)	1	
4	4	s	5105.98758	(036)	4		5081.81570	(000)	1	
5	0	a					5259.79245	(098)	3	N
5	0	s					5260.04662	(056)	3	N
5	1	a	5261.71468	(006)	2		5251.89534	(004)	3	N
5	1	s	5252.20730	(000)	1		5253.99682	(068)	3	N
5	2	a	5247.20506	(017)	2		5236.48427	(013)	3	N
5	2	s	5246.34567	(000)	2		5236.60008	(039)	4	N
5	3	a	5231.49862	(069)	3		5213.54848	(055)	2	N
5	3	s	5230.71631	(050)	3		5213.49259	(043)	2	N
5	4	a	5207.38235	(063)	3		5182.88251	(000)	1	N
5	4	s	5206.52591	(006)	3		5182.62268	(000)	2	N
5	5	a	5175.08813	(012)	2		5145.02734	(000)	1	
5	5	s	5174.05178	(024)	2		5143.88229	(000)	1	
6	0	a								
6	0	s	5382.22001	(028)	2	N				
6	1	a	5369.26516	(000)	1		5373.03376	(040)	2	N
6	1	s	5381.82808	(028)	3		5373.63126	(080)	3	N
6	2	a	5366.30856	(018)	2		5357.35257	(095)	3	N
6	2	s	5365.46875	(072)	2		5358.36937	(000)	1	N

Table 6 Continued

J'	K'	sym	E' cm ⁻¹	rms	n	E' cm ⁻¹	rms	n
l = + 1						l = -1		
6	3	a	5351.18041	(032)	3	5334.00995	(044)	3 N
6	3	s	5350.46750	(072)	3	5334.56963	(000)	1 N
6	4	a	5327.46920	(029)	3	5303.00022	(022)	4 N
6	4	s	5326.75854	(074)	3	5303.58511	(038)	2 N
6	5	a	5295.49114	(075)	3	5264.37192	(038)	2 N
6	5	s	5294.67264	(131)	2	5264.82734	(007)	2 N
6	6	a	5255.30808	(009)	2	5219.31180	(000)	1
6	6	s	5254.29499	(018)	2	5218.15277	(000)	1
7	1	a				5514.64768	(093)	3 N
7	1	s						
7	2	a	5504.89408	(000)	1			
7	2	s	5504.25101	(130)	2 N			
7	3	a	5490.35091	(103)	2 N			
7	3	s	5489.65497	(006)	2 N			
7	4	a	5467.14142	(066)	3 N	5443.74446	(064)	5 N
7	4	s	5466.52263	(087)	2 N	5443.22483	(000)	1 N
7	5	a	5435.61385	(057)	2 N	5403.62991	(013)	4 N
7	5	s	5434.90185	(205)	2 N	5404.24473	(008)	3 N
7	6	a	5395.73118	(020)	2 N	5359.56137	(000)	1 N
7	6	s	5394.93053	(008)	2 N	5359.28649	(056)	3 N
7	7	a	5348.91849	(158)	2 N	5305.80640	(000)	1
7	7	s	5347.67049	(006)	2 N	5304.64312	(033)	3
8	2	a	5662.46892	(045)	2 N			
8	2	s	5661.90803	(042)	2 N			
8	3	a	5648.95049	(085)	3 N			
8	3	s	5648.20991	(130)	2 N			
8	4	a	5626.32,631	(013)	2 N			
8	4	s	5625.70102	(053)	2 N			
8	5	a	5595.34210	(000)	1 N			
8	5	s	5594.73705	(000)	1 N			
8	6	a	5555.61142	(034)	2 N			
8	6	s	5555.02653	(044)	3 N			
8	8	a	5452.13038	(030)	2 N	5404.79601	(000)	1
8	8	s				5403.51481	(000)	1
9	3	a	5826.56550	(265)	2 N			
9	3	s	5826.20837	(000)	1 N			
9	6	a	5734.84334	(020)	3 N			
9	6	s	5734.36516	(012)	2 N			
9	8	a				5581.86780	(000)	1 N
9	8	s				5581.74862	(000)	1 N
9	9	a				5512.41850	(000)	1 N
9	9	s				5511.87148	(000)	1 N
10	6	a	5933.13022	(000)	1 N			
10	6	a	5933.47904	(054)	2 N			

Table 7 Comparison of Ammonia Band Centers in cm^{-1}

$^{14}\text{N } \nu_1 + \nu_4$	$^{14}\text{N } \nu_3 + \nu_4$	$^{15}\text{N } \nu_3 + \nu_4$	$\Delta[^{14}\text{N} - ^{15}\text{N}]$
4956.9122 a	5053.2346 a	5041.8706 a	11.3640
4955.7556 s	5052.6289 s	5041.2454 S	11.3835

Table 8 Summary of the 1996 HITRAN NH₃ Parameters at 2 μm

BAND	SYM	ISO	#LINES	Fmin	Fmax	Imin	Imax	Int-Sum
v ₁ +v ₄	a	1	122	4791.3	5128.6	2.0E-23	1.9E-21	1.599E-20
v ₁ +v ₄	s	1	112	4791.7	5111.1	2.1E-23	6.5E-22	1.471E-20
v ₃ +v ₄	a	1	272	4803.9	5293.0	6.1E-24	1.1E-20	3.121E-19
v ₃ +v ₄	s	1	264	4842.1	5293.6	2.2E-23	1.1E-20	3.199E-19
v ₃ +v ₄	a	2	63	4944.5	5179.8	3.1E-24	2.0E-21	3.389E-21
v ₃ +v ₄	s	2	66	4944.8	5158.7	3.1E-24	2.7E-22	1.024E-21
unassigned		1	1101	4802.2	5294.5	3.0E-24	3.6E-21	9.902E-20
#LINES	Fmin	Fmax	#ISO	#VIB	#BANDS	Int-Total		
2000	4791.3	5293.6	2	2	6	7.661E-19		

* The range of positions (Fmin, Fmax) are in units of cm⁻¹ and the intensities (Imin, Imax, Int-Sum, Int-Total) are in cm⁻¹/ (molecule-cm-2) near 296 K. 1 isotope number 1 and 2 are for ¹⁴NH₃ and ¹⁵NH₃, respectively. An isotopic abundance of 0.0035 has been assumed for ¹⁵N₃.

Table 9 Summary of NH₃ Intensity Measurements in Four Regions

Band	Center cm ⁻¹	S _v (fitted) Literature	Empirical Int. Sum
a 3v ₂ s v ₂ +v ₄ a v ₂ +v ₄ s 3v ₂ unassigned	2384.1 2540.5 2586.1 2895.5 —	0.61 (3) 0.186 (30) 0.174 (25) 0.244 (7) —	 0.175
s v, a s v ₃ a	3336.1 3337.1 3343.6 3344.0	 <u>22.27</u> (11) <u>13.1</u> (2.1)	
s v ₁ +v ₂ a s v ₂ +v ₃ a	4294.5 4320.0 4416.9 4435.4	 <u>2.71</u> <u>19.0</u>	
s v ₁ +v ₄ a v ₁ +v ₄ s v ₃ +v ₄ a v ₃ +v ₄ unassigned	4955.8 4956.9 5052.6 5053.2 —	 <u>17.19</u> —	0.396 0.364 = <u>0.760</u> 7.73 7.93 = <u>15.66</u> 2.45 18.99 = total

+ Intensities are in units of cm⁻²·atm⁻¹ at 296 K,

The data sources for S_v (fitted) are:

2600 cm⁻¹: Kleiner, Tarrago and Brown¹³; lit of 260 lines of 3v₂ and 466 lines of v₂+v₄,

3400 cm⁻¹: Pine and Dang-Nhu¹⁴; fit of 72 lines of v₁ and 19 lines of v₃

4400 cm⁻¹: Margolis and Kwan¹⁵; fit of 50 lines of v₁+v₂ and 170 lines of v₂+v₃

5000 cm⁻¹: Sarangi³; fit of 291 lines.

The empirical intensity summations are based on the Kleiner et al. and present Kitt Peak data.